

Cobalt/Mercury Carbide Clusters Based on Trigonal-Prismatic or Octahedral Co_6C Skeletons – X-ray Crystal Structure of $(\text{NEt}_4)_2[\text{Co}_6\text{C}(\text{CO})_{12}\{\text{HgW}(\text{CO})_3\text{Cp}\}_2]$

Roser Reina,^[a] Olga Riba,^[a] Oriol Rossell,^[a] Miquel Seco,^{*[a]} Dominique de Montauzon,^[b] Mercè Font-Bardia,^[c] and Xavier Solans^[c]

Keywords: Carbonyl complexes / Cluster compounds / Cobalt / Mercury / Rearrangements

The anionic transition metal clusters $(\text{NEt}_4)[\text{Co}_6\text{C}(\text{CO})_x\text{-}\{\text{HgM}\}]$ [$\text{M} = \text{W}(\text{CO})_3\text{Cp}$, $\text{Mo}(\text{CO})_3\text{Cp}$, $\text{Fe}(\text{CO})_2\text{Cp}$, $\text{Co}(\text{CO})_4$, $\text{Mn}(\text{CO})_5$] ($x = 13$ or 15) have been obtained by reaction of the corresponding octahedral ($x = 13$) or trigonal-prismatic ($x = 15$) cobalt carbido carbonyl clusters with the mercury

derivatives ClHgM . Metal skeleton rearrangements and some redox processes have been found to be induced by varying both the temperature and the solvent, resulting in new compounds containing tetra- or hexacoordinated mercury atoms.

Introduction

The fact that the mercury units HgM^+ [$\text{M} =$ a metal fragment such as $\text{Mo}(\text{CO})_3\text{Cp}$] can readily be attached to a wide variety of transition metal cluster anions has stimulated their use as general building blocks in the systematic synthesis of heterometallic clusters. In general, *typical* μ_2 - and μ_3 - HgM modes are found for a large number of polynuclear metal carbonyl clusters, where the mercury fragments bridge metal-metal edges or cap triangular faces of cluster cores.^[1] Two-centre two-electron bonding is found only for the simplest bi- and trimetallic compounds.^[2]

In comparison with other transition metals, only very few cobalt/mercury systems have been reported to date. This is surprising because cobalt and rhodium, for example, are unique in forming two hexanuclear anions with different metal frameworks, the octahedral $[\text{M}_6\text{C}(\text{CO})_{13}]^{2-}$ (86 EC) and the trigonal-prismatic $[\text{M}_6\text{C}(\text{CO})_{15}]^{2-}$ (90 EC), which can be interconverted through the uptake and release of carbon monoxide.^[3–5] This process can be rationalized in terms of a trigonal-twist mechanism, which involves the mutual rotation of the two triangles of metal atoms.

These considerations prompted us to explore the possibility of incorporating HgM^+ units into both of the aforementioned hexacobalt frameworks and to identify skeletal isomers. We were also interested in extending our studies to the investigation of potential skeletal rearrangements involving the new mercury/cobalt systems thus synthesized.

Results and Discussion

The selected ClHgM species [$\text{M} = \text{W}(\text{CO})_3\text{Cp}$, $\text{Mo}(\text{CO})_3\text{Cp}$, $\text{Fe}(\text{CO})_2\text{Cp}$, $\text{Co}(\text{CO})_4$, $\text{Mn}(\text{CO})_5$] were reacted separately with the NEt_4^+ salts of the anions $[\text{Co}_6\text{C}(\text{CO})_{15}]^{2-}$ (**1**) and $[\text{Co}_6\text{C}(\text{CO})_{13}]^{2-}$ (**2**) (see Scheme 1).

Reactions with the Trigonal-Prismatic $[\text{Co}_6\text{C}(\text{CO})_{15}]^{2-}$ Anion (**1**)

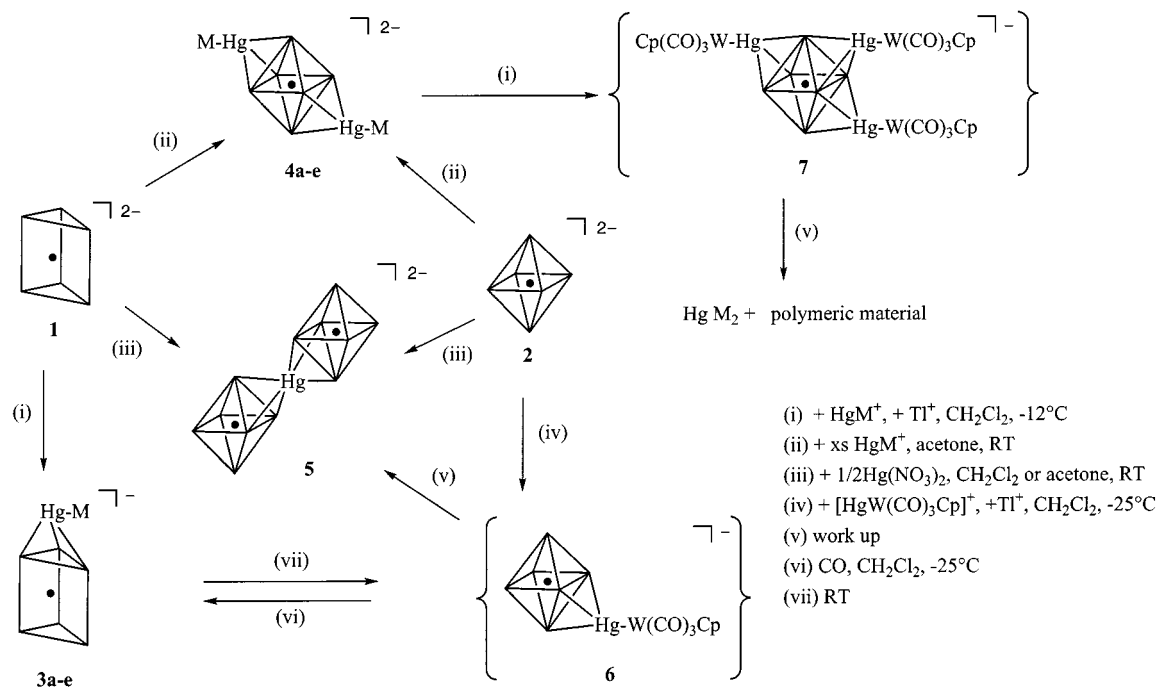
Treatment of $(\text{NEt}_4)_2[\text{Co}_6\text{C}(\text{CO})_{15}]$ (**1**) with ClHgM in CH_2Cl_2 at -12°C in the presence of a thallium salt as a halide abstractor gave the brown cluster complexes $(\text{NEt}_4)[\text{Co}_6\text{C}(\text{CO})_{15}\{\text{HgM}\}]$ [$\text{M} = \text{W}(\text{CO})_3\text{Cp}$ (**3a**), $\text{Mo}(\text{CO})_3\text{Cp}$ (**3b**), $\text{Fe}(\text{CO})_2\text{Cp}$ (**3c**), $\text{Co}(\text{CO})_4$ (**3d**), $\text{Mn}(\text{CO})_5$ (**3e**)]. Only compound **3a** could be isolated as a crystalline solid; the other mercury derivatives were recovered as oily materials. The $\nu(\text{CO})$ patterns in the IR spectra of **3a–e** were found to be almost superimposable if the bands due to the M part were ignored. The $\nu(\text{CO})$ bands are shifted to higher wavenumbers (by 30 cm^{-1}), indicating a decrease in electron density at the cobalt atoms. The observation of the ^{13}C NMR signal due to the carbide carbon atom at $\delta = 357$ confirmed that the incorporation of the mercury fragment does not induce a dramatic rearrangement of the metal framework. Mass spectrometry showed that the trigonal-prismatic Co_6C skeleton was preserved following the attachment of the mercury units. Thus, the parent molecular peak $[\text{M}^-]$ was observed for all the compounds, except in the case of the mercury/cobalt complex **3d**, where the most intense peak corresponded to $[\text{M} - 2\text{CO}]$.

In light of these data, we propose a molecular structure for type **3** complexes consisting of a triangular prism of cobalt atoms where one of the triangular faces, corresponding to the most basic sites on the prism surface,^[6] is capped by the mercury atom. In fact, this is the structure found for the analogous cluster anion of rhodium

^[a] Departament de Química Inorgànica, Universitat de Barcelona, Diagonal, 647, 08028 Barcelona, Spain
Fax: (internat.) + 34-93/490-7725
E-mail: miquel.seco@qi.ub

^[b] Laboratoire de Chimie de Coordination du CNRS, 205 route de Narbonne, 31077 Toulouse Cedex, France

^[c] Departament de Cristallografia, Mineralogia i Dipòsits Minerals, Universitat de Barcelona, Martí i Franquès s/n, 08028 Barcelona, Spain



Scheme 1

$[\text{Rh}_6\text{C}(\text{CO})_{15}\{\text{AuPR}_3\}]^-$ ($\text{R} = \text{Ph}, \text{Et}$),^[7,8] which is not surprising in view of the well-known isolobal relationship between the fragments AuPPh_3 and HgM .^[9] This implies, albeit with some exceptions, that both units occupy the same sites of a given cluster.^[10] The remaining negative charge suggested the possibility of introducing another mercury unit into these type 3 complexes. In fact, the reaction of **3** with ClHgM in a 1:1 molar ratio yielded a highly insoluble material that could not be characterized, along with the trimetallic species HgM_2 . The formation of these two products can be rationalized in terms of a rapid ligand-redistribution process of the initially formed $[\text{Co}_6\text{C}(\text{CO})_{15}(\text{HgM})_2]$. This result is in agreement with our predictions that the neutral mercury/transition metal clusters should be unstable with regard to the symmetrization process, while the negatively charged species should be reasonably stable and hence isolable in most cases.^[11]

In order to avoid the formation of oily materials and to determine whether the solvent plays an important role in our reactions, we allowed the $[\text{Co}_6\text{C}(\text{CO})_{15}]^{2-}$ anion (**1**) to react with ClHgM in acetone at room temperature. Surprisingly, under these conditions, we were able to isolate brown crystals of $(\text{NEt}_4)_2[\text{Co}_6\text{C}(\text{CO})_{12}\{\text{HgM}\}_2]$ [$\text{M} = \text{W}(\text{CO})_3\text{Cp}$ (**4a**), $\text{Mo}(\text{CO})_3\text{Cp}$ (**4b**), $\text{Fe}(\text{CO})_2\text{Cp}$ (**4c**), $\text{Co}(\text{CO})_4$ (**4d**), $\text{Mn}(\text{CO})_5$ (**4e**)] in moderate yields, accompanied by Co^{II} salts. These complexes were characterized by elemental analyses, spectroscopic data, and mass spectrometry. Their $\nu(\text{CO})$ bands were found to be shifted to lower frequencies by around 20 cm^{-1} , which is consistent with an increase in the electron density at the cobalt atoms. Their ^{13}C NMR spectra featured signals corresponding to the CO and Cp ligands, but the carbide signal was not observed. For all the

clusters of type **4**, FABMS showed the $[\text{M} + \text{H}]^-$ peak in accordance with the formula $[\text{Co}_6\text{C}(\text{CO})_{12}\{\text{HgM}\}_2]^{2-}$.

The structure of **4a** was confirmed by X-ray analysis. The geometry of the anion is shown in Figure 1, together with the atom numbering scheme. Selected bond lengths and angles are listed in Table 1.

The structure of this complex is based on that of the parent $[\text{Co}_6\text{C}(\text{CO})_{13}]^{2-}$ anion and has the two $\text{HgW}(\text{CO})_3\text{Cp}$ groups capping opposite faces of the distorted Co_6 octahedron. All the other edges are bridged by CO ligands to give a symmetrical structure with the central carbon atom at a crystallographic centre of symmetry. Each cobalt atom bears a terminal carbonyl ligand. As expected, the mercury coordination to the Co_3 faces causes an appreciable lengthening of the distances between these cobalt atoms (average 2.806 \AA). The Hg atom resides in a strongly distorted tetrahedral arrangement involving the three Co atoms and the W atom. The $\text{HgW}(\text{CO})_3\text{Cp}$ moiety shows the usual four-legged piano stool arrangement with a W–Hg distance of $2.781(2)\text{ \AA}$.

The coordination of this unit does not lead to any appreciable expansion of the Co_6C octahedron, and the distances between the carbido carbon atom and the cobalt atoms (average 1.873 \AA) remain similar to those observed in the $[\text{Co}_6\text{C}(\text{CO})_{13}]^{2-}$ anion [average $1.87(1)\text{ \AA}$].

The Co–Hg distances (average 2.717 \AA) are shorter than those observed in other $\text{Co}_3(\mu_3\text{-HgR})$ systems, e.g. $[\text{FeCo}_3(\text{CO})_{12}\{\mu_3\text{-HgMo}(\text{CO})_3\text{Cp}\}]$ (average 2.816 \AA) and $[\text{RuCo}_3(\text{CO})_{12}\{\mu_3\text{-HgCo}(\text{CO})_4\}]$ (average 2.756 \AA).^[12] The Co_6Hg_2 metal framework found for **4a** has no precedent in the chemistry of the Group 9 elements. Its formation re-

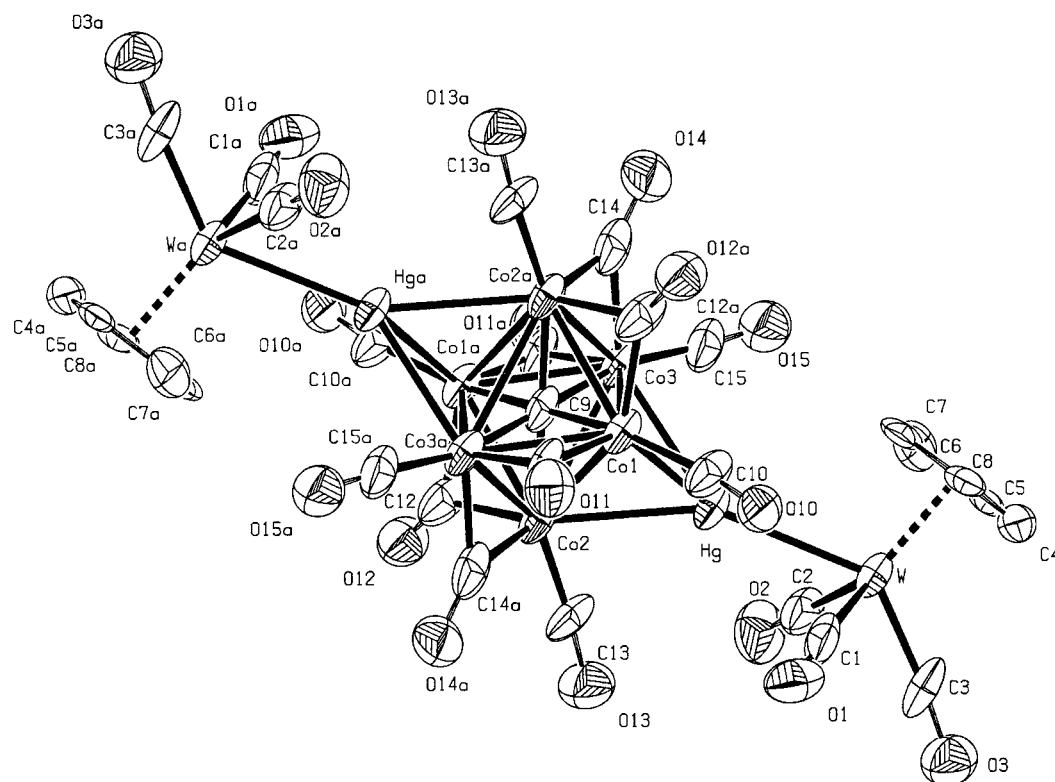


Figure 1. View of the molecular structure of the cluster anion $[\text{Co}_6\text{C}(\text{CO})_{12}\{\mu_3\text{-HgW}(\text{CO})_3\text{Cp}\}_2]^{2-}$ (anion of **4a**) showing the atom numbering scheme

Table 1. Selected bond lengths [Å] and angles [deg] in **4a**

Co(1)–Co(2)	2.799(2)
Co(1)–Co(3)	2.832(2)
Co(2)–Co(3)	2.789(3)
Co(1)–Co(2a)	2.489(2)
Co(1)–Co(3a)	2.470(2)
Hg–Co(3)	2.711(2)
Hg–Co(2)	2.716(2)
Hg–Co(1)	2.7261(19)
Co(1)–C(10)	1.720(9)
Co(1)–C(11)	1.869(11)
Co(1)–C(9)	1.8823(16)
Co(2)–C(13)	1.707(9)
Co(2)–C(9)	1.8633(17)
Co(2)–C(12)	1.905(9)
Co(3)–C(15)	1.682(11)
Co(3)–C(9)	1.8751(19)
Co(3)–C(14)	1.909(10)
Co(3)–Co(1a)	2.470(2)
Co(3)–Co(2a)	2.489(2)
Co(2)–Hg–Co(1)	61.90(6)
Co(3)–Hg–Co(2)	61.86(6)
Co(3)–Hg–Co(1)	62.77(6)
Co(3)–Co(2)–Co(1)	60.89(5)
Co(2)–Co(3)–Co(1)	59.72(6)
Co(2)–Co(1)–Co(3)	59.39(7)
Hg–Co(2)–Co(1)	59.23(4)
Hg–Co(1)–Co(2)	58.87(5)
Co(3)–Hg–Co(2)	61.86(6)
Co(2a)–C(9)–Co(3)	83.49(8)
Co(2)–C(9)–Co(1a)	83.30(7)
Co(3)–C(9)–Co(1a)	82.19(7)
Co(3)–C(9)–Co(1)	97.81(7)
Co(3)–Hg–W	138.95(5)
Co(2)–Hg–W	151.96(4)
Co(1)–Hg–W	138.32(5)

quires the loss of three carbonyl ligands from the starting anion in order to permit both the skeletal rearrangement from the prism to the octahedron and the redox process that gives the double negative charge on the cluster. Considering that each HgM fragment contributes 12 electrons to the polyhedral electron count of the cluster, compound **4** conforms to the number of electrons (110) expected for a bicapped octahedron according to the condensation rules given by polyhedral skeletal electron-pair theory.^[13] It is noteworthy that the formation of **4**, possessing a Co₆ octahedral core, proceeds through a skeletal rearrangement of the trigonal prism $[\text{Co}_6\text{C}(\text{CO})_{15}]^{2-}$ resulting from the incorporation of two mercury units. This structural feature has not previously been observed in the chemistry of rhodium. For example, the reaction of $[\text{Rh}_6\text{C}(\text{CO})_{15}]^{2-}$ with two equivalents of ClAuPPh_3 affords $[\text{Rh}_6\text{C}(\text{CO})_{15}\{\text{AuPPh}_3\}_2]^{2-}$,^[7] which displays a trigonal-prismatic framework of Rh atoms capped on both triangular faces by a gold atom. It is clear that in the present case the driving force for the skeletal rearrangement is the energy involved in the formation of the three new Co–Co bonds as well as three extra Co–Hg bonds and the entropic contribution from the liberation of the three CO ligands required in the transformation of the trigonal prism to the octahedral core. On the other hand, steric interactions between the terminal and in-plane edge-bridging carbonyl ligands and the incoming mercury fragments should not be ruled out as an influence on the skeletal rearrangement process.

In an attempt to obtain other cobalt clusters possessing trigonal-prismatic skeletons, we tried to synthesize $[\text{Hg}\{\text{Co}_6\text{C}(\text{CO})_{15}\}_2]^{2-}$ by reacting the starting cobalt anion $[\text{Co}_6\text{C}(\text{CO})_{15}]^{2-}$ (**1**) with $\text{Hg}(\text{NO}_3)_2$ in a 2:1 molar ratio in CH_2Cl_2 or acetone at room temperature (see Scheme 1). However, the spectroscopic data of the brown crystals thus obtained indicated that the new compound was actually $[\text{Hg}\{\text{Co}_6\text{C}(\text{CO})_{13}\}_2]^{2-}$ (**5**). ^{13}C NMR spectroscopy proved to be an excellent tool for determining the geometry of the cobalt core: the carbide carbon atom gives rise to a signal at $\delta \approx 460$ when it is at the centre of the octahedron or at $\delta \approx 350$ when it resides within the trigonal prism. In the case of **5**, the ^{13}C NMR spectrum features a signal at $\delta = 466$, suggesting a metal framework based on a six-coordinate mercury atom capping one triangular face of two octahedra. Consequently, the coordination about mercury can be described as octahedral, which is rather unusual in the organometallic chemistry of this element.^[14]

Reactions with the Octahedral $[\text{Co}_6\text{C}(\text{CO})_{13}]^{2-}$ Anion (**2**)

When a solution of $(\text{NEt}_4)_2[\text{Co}_6\text{C}(\text{CO})_{13}]$ (**2**) in CH_2Cl_2 was treated with $\text{ClHgW}(\text{CO})_3\text{Cp}$ (1:1 molar ratio) at -25°C in the presence of a thallium salt, the IR spectrum of the solution showed a shift of the carbonyl bands to higher wavenumbers (by around 40 cm^{-1}), indicating the attachment of the mercury fragment to the skeleton of the cobalt anion. Efforts to isolate the expected product $(\text{NEt}_4)[\text{Co}_6\text{C}(\text{CO})_{13}\{\text{HgW}(\text{CO})_3\text{Cp}\}]$ (**6**) were unsuccessful; after workup of the solution we could only separate HgM_2 along with crystals of $(\text{NEt}_4)_2[\text{Hg}\{\text{Co}_6\text{C}(\text{CO})_{13}\}_2]$ (**5**), the identity of which was established by comparison with an authentic sample obtained from the reaction of $[\text{Co}_6\text{C}(\text{CO})_{13}]^{2-}$ (**2**) with $\text{Hg}(\text{NO}_3)_2$ (see Scheme 1). In view of the fact that it proved impossible to isolate compound **6**, we submitted a fresh reaction solution in CH_2Cl_2 to mass spectrometric analysis in order to confirm the formation of the desired complex. We thus observed the parent molecular peak, $[\text{M}]^-$, corresponding to the formula $[\text{Co}_6\text{C}(\text{CO})_{13}\{\text{HgW}(\text{CO})_3\text{Cp}\}]^-$.

The question that arises is the mechanism by which **5** is formed in the above reaction. The simultaneous formation of the symmetrical species in the course of the reaction suggests that **5** is formed from the nonisolated species **6** by slow ligand redistribution. Despite the fact that $[\text{Co}_6\text{C}(\text{CO})_{13}\{\text{HgW}(\text{CO})_3\text{Cp}\}]^-$ bears one negative charge and, consequently, is relatively inert to symmetrization processes, with high nuclearity clusters a spontaneous albeit slow symmetrization occasionally takes place.^[15,16] The failure to isolate **6** precluded its spectroscopic characterization. However, it was thought that the addition of four electrons to its polyhedral skeleton, by reaction with carbon monoxide, would facilitate skeletal arrangement to the trigonal-prismatic $[\text{Co}_6\text{C}(\text{CO})_{15}\{\text{HgW}(\text{CO})_3\text{Cp}\}]^-$ (**3a**), which has been characterized previously. Indeed, compound **6** was found to react with a smooth stream of CO at -25°C to give **3a**, thus confirming our expectations. Interestingly, when the reaction mixture was allowed to warm to room temperature, reversion to **6** was noted. Bearing in mind the

isolobal relationship between HgM and AuPPh_3 , and the fact that the crystal structure of the anion $[\text{Co}_6\text{C}(\text{CO})_{13}\{\text{AuPPh}_3\}]^-$ has recently been determined,^[17] we propose a similar metal core for **6** consisting of a cobalt octahedron capped at a triangular face by the mercury atom.

The importance of the nature of the solvent as well as the temperature was again evidenced in the reaction of $[\text{Co}_6\text{C}(\text{CO})_{13}]^{2-}$ (**2**) with HgM^+ . When the reaction was carried out in acetone at room temperature, moderate yields of type **4** complexes were obtained. Their formation from the octahedral cobalt anion involves the loss of one carbonyl ligand according to an as-yet-unclear mechanism. Taking into account the dianionic character of type **4** compounds and their relative stability, we decided to test their reactivity further. When **4a** was reacted with another equivalent of $\text{ClHgW}(\text{CO})_3\text{Cp}$ in CH_2Cl_2 at -12°C in the presence of a thallium salt, the expected monoanionic $[\text{Co}_6\text{C}(\text{CO})_{12}\{\text{HgW}(\text{CO})_3\text{Cp}\}_3]^-$ species **7** could be detected in solution by IR spectroscopy as well as by mass spectrometry (ESMS), where the parent molecular peak was observed. Unfortunately, however, after workup the isolated products were $\text{Hg}[\text{W}(\text{CO})_3\text{Cp}]_2$ and a highly insoluble, intractable material. This behaviour would suggest that the incoming third metal fragment promotes a spontaneous symmetrization reaction.

In conclusion, we have shown that both hexanuclear cobalt clusters react with mercury halide complexes to give mono- and di-capped trigonal prisms or octahedral skeletons. The tendency of the more open trigonal-prismatic cores to rearrange into an octahedral geometry would seem to indicate that the latter metal framework is the most stable for mixed mercury/cobalt clusters.

Electrochemical Studies

The electrochemical properties of these compounds were studied in the electroactivity range of the solvent (CH_2Cl_2) to compare the electrochemical behaviour of the octahedral and prismatic geometry complexes, as well as to allow comparison with related compounds.

The Co_6 -based prismatic complex **3a** showed a one-electron irreversible reduction step at $E_{\text{p,c}} = -0.80\text{ V}$ and a one-electron reversible oxidation step at $E^\circ = 0.66\text{ V}$ (see Table 2), but the instability of the compound did not permit a mechanistic study of its electrochemical processes.

Owing to the rapid decomposition of the cluster **4c** in solution, no electrochemical study could be carried out. The other dianionic octahedral clusters with different mercury fragments showed a reversible reduction at around -1.2 V , except for the cobalt derivative **4d**, for which the reduction step was irreversible. These species were also seen to undergo an irreversible oxidation at around 0.2 V when the scan rate was 0.1 Vs^{-1} , but it became a quasi-reversible process at a scan rate of 0.5 Vs^{-1} (Table 2). The oxidation was a one-electron step, as shown by comparison with the height of the reduction wave (due to passivation phenomena, reliable coulometry could not be performed). When the oxidation was carried out in an EPR tube with $[\text{FeCp}_2][\text{PF}_6]$

Table 2. Cyclic voltammetry data

[a] compd.	Reduction		<i>i</i> _{p,c} / <i>i</i> _{p,a}	<i>n</i>	Oxidation		<i>i</i> _{p,a} / <i>i</i> _{p,c}	<i>n</i>
	<i>E</i> ^{o'} [V]	Δ <i>E</i> [mV]			<i>E</i> ^{o'} [V]	Δ <i>E</i> [mV]		
3a	−0.80 ^[b]			1	0.66	136	0.59	1
4a	−1.30	70	1.03	1	0.18 ^[c]			1
4b	−1.23	73	0.99	1	0.25 ^[c]			1
4d	−1.10 ^[b]			1	0.43 ^[c]			1
4e	−1.24	122	0.74	1	0.32 ^[c]			1
5	−0.55	88	0.80	1	0.26 ^[c]			1
	−0.88	123	1.15	1				

[a] Scan rate: 0.1 Vs^{−1} vs. SCE in 0.1 M Bu₄NBF₄ in CH₂Cl₂ or acetone at −15 °C. — [b] *E*_{p,c} (irreversible reduction). — [c] *E*_{p,a} (irreversible oxidation).

in CH₂Cl₂ at −78 °C, the radical species [Co₆C(CO)₁₂{HgM}₂]^{•−} was detected. The X-band EPR spectrum consists of a single strong resonance centred at ca. 3373 G (*g* = 2.0028). The identities of the decomposition products were verified by IR spectroscopy.

Compound **5** shows a one-electron irreversible oxidation step at *E*_{p,a} = 0.26 V (controlled potential coulometry at 0.3 V). Moreover, this cluster was seen to undergo two well-defined one-electron reversible reductions at *E*^{o'} = −0.55 V and *E*^{o'} = −0.88 V by comparison of the wave heights with that for the oxidation step (Table 2). The instability of this compound in solution and the passivation phenomena at the electrode surface precluded a supplementary electrochemical study.

In summary, we have observed that those compounds which adopt an octahedral geometry exhibit reversible reduction steps, while the prismatic cluster shows an irreversible reduction wave. This behaviour compares well with the irreversible reduction steps found for the prismatic [Co₆C(CO)₁₅]^{2−} starting dianion.^[19]

Conclusions

Reaction of the [Co₆C(CO)₁₅]^{2−} and [Co₆C(CO)₁₃]^{2−} anions with one mol of HgM⁺ gives the octanuclear species [Co₆C(CO)₁₅{HgM}][−] and [Co₆C(CO)₁₃{HgM}][−], having spiked Co₆C trigonal-prismatic and spiked octahedral skeletons, respectively. These species can be interconverted through the addition or elimination of CO. On the other hand, the use of an excess of HgM⁺ has been found to lead invariably to the cluster [Co₆C(CO)₁₂{HgM}₂]^{2−}, in which the Co₆C octahedron is doubly-capped by HgM⁺ moieties. Finally, electrochemical studies on the dimercury complexes have revealed that their oxidation leads to radical species [Co₆C(CO)₁₂{HgM}₂]^{•−}, which could be detected by EPR.

Experimental Section

General: All manipulations were performed under an atmosphere of purified N₂ using standard Schlenk techniques. All solvents were distilled from appropriate drying agents. — Infrared spectra were recorded from samples in CH₂Cl₂ or acetone solution on a Nicolet

FT-IR 520 spectrophotometer. — ¹H, ¹³C{¹H}, and ³¹P{¹H} NMR spectra were recorded on Bruker DRX 250 and Varian XL-500 spectrometers and were referenced to TMS (δ_H, δ_C = 0.0) and 85% H₃PO₄ (δ_P = 0.0). — FAB and ES mass spectra were recorded on a Fisons VG Quattro spectrometer with samples injected as CH₂Cl₂, methanol, or acetone solutions. — EPR spectra were obtained on a Bruker ESP 300 E spectrometer operating in the X-band mode at 100 K, as maintained by a standard Bruker VT 1000 cryostat. — The compounds ClHgM^[20] [M = Mo(CO)₃Cp, W(CO)₃Cp, Fe(CO)₂Cp, Co(CO)₄, Mn(CO)₅], (NEt₄)₂[Co₆C(CO)₁₅]^[6] and (NEt₄)₂[Co₆C(CO)₁₃]^[3] were synthesized as described previously. The synthetic methodology detailed in this section corresponds to the reactions described in Scheme 1 that afforded better yields and pure final products. The elemental analyses for compounds **3b–e** are not reported because they did not burn properly in the analyser.

Synthesis of (NEt₄)₂[Co₆C(CO)₁₅{μ-HgM}] [M = W(CO)₃Cp (**3a**), Mo(CO)₃Cp (**3b**), Fe(CO)₂Cp (**3c**), Co(CO)₄ (**3d**), Mn(CO)₅ (**3e**)]: Details of the synthesis of **3a** also apply to **3b–e**, although the latter were obtained as oily materials. To a precooled solution of (NEt₄)₂[Co₆C(CO)₁₅] (**1**) (0.30 g, 0.28 mmol) in CH₂Cl₂ (15 mL) at −12 °C were added solid ClHgW(CO)₃Cp (0.16 g, 0.28 mmol) and TIBF₄ (0.09 g, 0.28 mmol). After stirring for 10 min, the starting material had been consumed and the mixture was filtered to remove the salts. The filtrate was layered with pentane (5 mL). Storage at −30 °C for 8 h resulted in the deposition of **3a** as a brown crystalline solid (0.15 g, 37% yield). — IR (CH₂Cl₂): $\tilde{\nu}$ (ν_{CO} stretch) = 2053 cm^{−1} m, 2011 vs, 1963 s, 1889 m, 1856 m. — ¹H NMR (295 K, CD₂Cl₂): δ = 1.3 (tt, 12 H, CH₃), 3.2 (q, 8 H, CH₂), 5.5 (s, 5 H, C₅H₅). — ¹³C NMR (295 K, CD₂Cl₂): δ = 7.3 (s, CH₃), 53.0 (s, CH₂), 86.9 (s, C₅H₅), 357.0 (s, C). — FABMS: *m/z* = 1318 [M[−]]. — C₃₂H₂₆Co₆HgNO₁₆W (1449.58): C 26.51, H 1.74, N 0.97; found C 26.59, H 1.72, N 1.00.

3b: IR (CH₂Cl₂): $\tilde{\nu}$ (ν_{CO} stretch) = 2053 cm^{−1} m, 2007 vs, 1963 s, 1882 m, 1852 m. — ¹H NMR (295 K, CD₂Cl₂): δ = 1.3 (tt, 12 H, CH₃), 3.2 (q, 8 H, CH₂), 5.4 (s, 5 H, C₅H₅). — FABMS: *m/z* = 1233 [M[−]].

3c: IR (CH₂Cl₂): $\tilde{\nu}$ (ν_{CO} stretch) = 2069 cm^{−1} w, 2049 m, 2008 vs, 1925 w, 1857 m. — ¹H NMR (295 K, CD₂Cl₂): δ = 1.32 (tt, 12 H, CH₃), 3.2 (q, 8 H, CH₂), 4.7 (s, 5 H, C₅H₅). — FABMS: *m/z* = 1164 [M[−]].

3d: IR (CH₂Cl₂): $\tilde{\nu}$ (ν_{CO} stretch) = 2063 cm^{−1} m, 2049 m, 2011 vs, 1849 m. — FABMS: *m/z* = 1103 [M[−] − 2CO].

3e: IR (CH₂Cl₂): $\tilde{\nu}$ (ν_{CO} stretch) = 2070 cm^{−1} w, 2047 m, 2010 vs, 1860 w. — ESMS: *m/z* = 1182 [M[−]].

Synthesis of (NEt₄)₂[Co₆C(CO)₁₂{μ₃-HgM}] [M = W(CO)₃Cp (**4a**), Mo(CO)₃Cp (**4b**), Fe(CO)₂Cp (**4c**), Co(CO)₄ (**4d**), Mn(CO)₅ (**4e**)]: The general procedure is described for the case of **4a**. To a solution of (NEt₄)₂[Co₆C(CO)₁₅] (**1**) (0.30 g, 0.28 mmol) in acetone (20 mL) at room temperature was added solid [ClHgW(CO)₃Cp] (0.16 g, 0.28 mmol). After the mixture had been stirred for 2 h, addition of a 30% excess of [ClHgW(CO)₃Cp] (0.05 g) was found to be necessary to complete the reaction. The reaction mixture was stirred for a further 2 h and then hexane (20 mL) was added in order to precipitate the salts. After filtration, the slow addition of further hexane (10 mL) under vigorous stirring led to the deposition of red-brown crystals of **4a** (0.18 g, 30% yield). — IR (acetone): $\tilde{\nu}$ (ν_{CO} stretch) = 2001 cm^{−1} w, 1962 vs, 1875 m, 1863 m, 1814 m. — ¹H NMR (295 K, [D₆]acetone): δ = 1.4 (tt, 24 H, CH₃), 3.5 (q, 16 H, CH₂), 5.3 (s, 10 H, C₅H₅). — ¹³C NMR (295 K, [D₆]acetone): δ = 7.5 (s, CH₃), 52.8 (s, CH₂), 88.6 (s, C₅H₅), 218.0 (m, CO), 237.5 (m, CO). — FABMS: *m/z* = 1768 [M + H][−]. — C₄₅H₅₀Co₆Hg₂N₂O₁₈W₂ (2029.37): C 26.61, H 2.48, N 1.37; found C 26.69, H 2.51, N 1.40.

For compounds **4b–e**, the addition of diethyl ether (20 mL) caused the precipitation of the salts. Indeed, all the crystalline solids were obtained with diethyl ether, although varying excesses of ClHgM, different reaction times, and modified final workup conditions were needed.

4b: 40% excess ClHgMo(CO)₃Cp; 2 h reaction time; the final precipitation was achieved by the addition of diethyl ether (20 mL) in aliquots of 5 mL. 0.14 g, 27% yield. – IR (acetone): $\tilde{\nu}$ (ν_{CO} stretch) = 2002 cm^{−1} w, 1964 vs, 1882 m, 1868 m, 1814 m. – ¹H NMR (295 K, [D₆]acetone): δ = 1.4 (tt, 24 H, CH₃), 3.5 (q, 16 H, CH₂), 5.2 (s, 10 H, C₅H₅). – ¹³C NMR (295 K, [D₆]acetone): δ = 7.5 (s, CH₃), 52.8 (s, CH₂), 89.9 (s, C₅H₅), 235.7–229.7 (m, CO). – FABMS: m/z = 1594 [M + H]⁺. – C₄₅H₅₀Co₆Hg₂N₂O₁₈Mo₂ (1853.55): C 29.16, H 2.72, N 1.51; found C 29.19, H 2.75, N 1.52.

4c: 25% excess ClHgFe(CO)₂Cp; 6 h reaction time; precipitation occurred after 8 h at −30 °C. 0.12 g, 25% yield. – IR (acetone): $\tilde{\nu}$ (ν_{CO} stretch) = 2053 cm^{−1} m, 1994 m, 1969 vs, 1908 w, 1891 w, 1816 m. – ¹H NMR (295 K, [D₆]acetone): δ = 1.4 (tt, 24 H, CH₃), 3.5 (q, 16 H, CH₂), 4.6 (s, 10 H, C₅H₅). – ¹³C NMR (295 K, [D₆]acetone): δ = 7.5 (s, CH₃), 52.8 (s, CH₂), 81.1 (s, C₅H₅), 214.2 (s, CO). – FABMS: m/z = 1458 [M + H]⁺. – C₄₃H₅₀Co₆Fe₂Hg₂N₂O₁₆ (1717.34): C 30.07, H 2.93, N 1.63; found C 30.11, H 2.95, N 1.65.

4d: 30% excess ClHgCo(CO)₄; 2 h reaction time; the final precipitation was accomplished by the addition of diethyl ether (20 mL) in aliquots of 5 mL. 0.12 g, 25% yield. – IR (acetone): $\tilde{\nu}$ (ν_{CO} stretch) = 2052 cm^{−1} m, 1977 vs, 1963 s, 1890 w, 1825 m. – ¹³C NMR (295 K, [D₆]acetone): δ = 7.5 (s, CH₃), 52.8 (s, CH₂), 209.7 (s, CO), 233.2 (m, CO). – FABMS: m/z = 1445 [M + H]⁺. – C₃₇H₄₀Co₈Hg₂N₂O₂₀ (1705.37): C 26.06, H 2.36, N 1.64; found C 26.09, H 2.37, N 1.66.

4e: 25% excess ClHgMn(CO)₅; 6 h reaction time; precipitation occurred after 8 h at −30 °C. 0.14 g, 28% yield. – IR (acetone): $\tilde{\nu}$ (ν_{CO} stretch) = 2062 cm^{−1} m, 1981 vs, 1954 s, sh, 1891 w, 1820 m. – ¹³C NMR (295 K, [D₆]acetone): δ = 7.5 (s, CH₃), 52.8 (s, CH₂), 218.1 (m, CO). – FABMS: m/z = 1493 [M + H]⁺. – C₃₉H₄₀Co₆Hg₂Mn₂N₂O₂₂ (1753.40): C 26.71, H 2.29, N 1.60; found C 26.73, H 2.32, N 1.62.

(NEt₄)₂[Hg{Co₆C(CO)₁₃}₂] (**5**): Solid Hg(NO₃)₂ (0.05 g, 0.15 mmol) was added to a solution of (NEt₄)₂[Co₆C(CO)₁₃] (**2**) (0.30 g, 0.30 mmol) in CH₂Cl₂ (20 mL). The mixture was stirred at room temperature for 5 h and then filtered. The resulting solution was layered with hexane (10 mL) and cooled overnight at −30 °C to give 0.16 g (30% yield) of a dark-brown crystalline solid. – IR (CH₂Cl₂): $\tilde{\nu}$ (ν_{CO} stretch) = 2037 cm^{−1} w, 2007 vs, 1844 w. – ¹³C NMR (295 K, CD₂Cl₂): δ = 7.8 (s, CH₃), 53.0 (s, CH₂), 219.5 (s, CO), 225.1 (s, CO), 466.0 (s, C). – FABMS: m/z = 1633 [M – CO]⁺. – ESMS: m/z = 830 [M/2]²⁺. – C₄₄H₄₀Co₁₂HgN₂O₂₆ (1922): C 25.14, H 0.95, N 1.33; found C 25.19, H 0.99, N 1.34.

Reaction of (NEt₄)₂[Co₆C(CO)₁₃] with ClHgW(CO)₃Cp – Formation of (NEt₄)₂[Co₆C(CO)₁₃{μ₃-HgW(CO)₃Cp}] (6**):** To a solution of (NEt₄)₂[Co₆C(CO)₁₃] (**2**) (0.30 g, 0.30 mmol) in CH₂Cl₂ (15 mL) at −25 °C were added solid ClHgW(CO)₃Cp (0.17 g, 0.30 mmol) and TIBF₄ (0.09 g, 0.30 mmol). The resulting mixture was stirred for 1 h. Subsequent addition of hexane (5 mL) caused the precipitation of the salts, which were filtered off. The IR and ES mass spectra of the resulting solution confirmed the formation of [Co₆C(CO)₁₃{μ₃-HgW(CO)₃Cp}][−] (**6**). – IR (CH₂Cl₂): $\tilde{\nu}$ (ν_{CO} stretch) = 2053 cm^{−1} m, 2004 vs, 1870 m, 1845 m. – ESMS: m/z = 1263 [M][−].

Reaction of (NEt₄)₂[Co₆C(CO)₁₂{μ-HgW(CO)₃Cp}]₂ with ClHgW(CO)₃Cp – Formation of (NEt₄)₂[Co₆C(CO)₁₂-

{HgW(CO)₃Cp}]₃] (7**):** To a solution of (NEt₄)₂[Co₆C(CO)₁₂{μ-HgW(CO)₃Cp}]₂ (**4a**) (0.25 g, 0.12 mmol) in CH₂Cl₂ (15 mL) at −12 °C were added solid [ClHgW(CO)₃Cp] (0.07 g, 0.12 mmol) and TIBF₄ (0.04 g, 0.12 mmol). The resulting mixture was stirred for 1 h. Subsequent addition of hexane (5 mL) caused the precipitation of the salts, which were filtered off. The IR and ES mass spectra of the resulting solution confirmed the formation of [Co₆C(CO)₁₂{μ-HgW(CO)₃Cp}]₃[−] (**7**). – IR (CH₂Cl₂): $\tilde{\nu}$ (ν_{CO} stretch) = 1993 cm^{−1} vs, 1962 s, 1878 m. – ESMS: m/z = 2303 [M][−].

Electrochemical Measurements: Electrochemical measurements were carried out using an Electrochemat potentiostat.^[21] Electrochemical experiments were performed at −15 °C with CH₂Cl₂ as a solvent, except in the case of compounds **4a–e**, in an airtight three-electrode cell connected to an argon line. The reference electrode consisted of a saturated calomel electrode (SCE), separated from the nonaqueous solutions by a bridge compartment. The counterelectrode was a spiral of platinum wire 8 cm in length and 0.5 cm in diameter with an apparent surface area of ca. 1 cm². The working electrode was an Au wire (0.125 mm diameter). For electrolysis, a gold wire (1 mm in diameter, 10 cm in length) or a platinum foil was used. $E^{\circ'}$ values were determined as the average of the cathodic and anodic peak potentials, i.e. (E_{pc} + E_{pa})/2. The supporting electrolyte (*n*Bu₄N)[BF₄] (Fluka, electrochemical grade) was used as received. Dichloromethane and acetone were freshly distilled prior to use. The solutions used for the electrochemical studies were typically 4 × 10^{−4} M in the cluster complex and 0.1 M in (*n*Bu₄N)[BF₄]. Under the same conditions, ferrocene was found to be oxidized at $E^{\circ'} = 0.42$ V vs. SCE and the peak potential separation ΔE was 60 mV. Cyclic voltammetry experiments were run at a scan rate of 0.1 Vs^{−1}.

X-ray Structure Determination of 4a: A prismatic crystal (0.1 × 0.1 × 0.2 mm) was selected and mounted on an Enraf–Nonius CAD4 four-circle diffractometer. Crystallographic and experimental details are summarized in Table 3. Unit cell parameters were determined from the automatic centring of 25 reflections (12 < θ < 21°) and refined by least-squares methods. Intensities were collected with graphite-monochromated Mo-*K*_α radiation using the ω/θ

Table 3. Crystal data and structure refinement for **4a**

Empirical formula	C ₄₅ H ₄₈ Co ₆ Hg ₂ N ₂ O ₁₈ W ₂
Formula weight	2027.31
Temperature	293(2) K
Wavelength	0.71069 Å
Crystal system, space group	monoclinic, <i>P</i> ₂ ₁ / <i>n</i>
Unit cell dimensions	<i>a</i> = 13.283(9) Å α = 90° <i>b</i> = 13.544(10) Å β = 101.75(5)° <i>c</i> = 15.409(10) Å γ = 90°
Volume	2714(3) Å ³
<i>Z</i>	2
Calculated density	2.481 Mg/m ³
Absorption coefficient	11.704 mm ^{−1}
<i>F</i> (000)	1892
Crystal size	0.1 × 0.1 × 0.2 mm
θ range for data collection	2.02 to 29.96°
Index ranges	−18 ≤ <i>h</i> ≤ 18 0 ≤ <i>k</i> ≤ 19 0 ≤ <i>l</i> ≤ 21
Reflections collected/unique	8354/7845 [<i>R</i> (int) = 0.0220]
Refinement method	Full-matrix least-squares on <i>F</i> ²
Data/parameters	7845/331
Goodness-of-fit on <i>F</i> ²	0.985
Final <i>R</i> indices [<i>I</i> > 2σ(<i>I</i>)]	<i>R</i> 1 = 0.0279, <i>wR</i> 2 = 0.0449
<i>R</i> indices (all data)	<i>R</i> 1 = 0.1091, <i>wR</i> 2 = 0.0732
Largest diff. peak and hole	0.616 and −0.597 e.Å ^{−3}

2 Θ scan technique. 8354 reflections were measured in the range $2.02 \leq \Theta \leq 29.96$, 7845 of which were nonequivalent by symmetry [R_{int} (on I) = 0.022]. 6478 reflections were considered as observed, applying the condition $I > 2\sigma(I)$. Three reflections were measured every two hours as an orientation and intensity control; no significant intensity decay was observed. Lorentz polarization but no absorption corrections were made.

The structure was solved by direct methods using SHELXS and refined by full-matrix least-squares methods with SHELX-97,^[22] using all 7845 nonequivalent reflections. Very negative intensities were discarded. The function minimized was $\Sigma w||F_o|^2 - |F_c|^2|^2$, where $w = [\sigma^2(I) + (0.0102P)^2]^{-1}$, and $P = (|F_o|^2 + 2|F_c|^2)/3$; f , f' , and f'' were taken from the International Tables of X-ray Crystallography.^[23]

The cyclopentadiene unit was refined with the C–C bond length and the C–C–C bond angle constrained to 1.420 Å and 108.0°. The final R (on F) factor was 0.027, wR (on $|F|^2$) = 0.044, and goodness of fit = 0.479 for all observed reflections. The number of refined parameters was 331. Max. shift/e.s.d. = 0.00, mean shift/e.s.d. = 0.00. Max. and min. peaks in final difference synthesis: 0.616 and -0.597 eÅ^{-3} , respectively.

Crystallographic data (excluding structure factors) for the structure reported in this paper have been deposited with the Cambridge Crystallographic Data Centre as supplementary publication no. CCDC-145260. Copies of the data can be obtained free of charge on application to the CCDC, 12 Union Road, Cambridge CB2 1EZ, U.K. [Fax: (internat.) +44-1223/336-033; E-mail: deposit@ccdc.cam.ac.uk].

Acknowledgments

This work was supported by the DGICYT (Project PB96–0174) and the CIRIT (Project 1997 SGR 00174).

^[1] L. H. Gade, *Angew. Chem. Int. Ed. Engl.* **1993**, *32*, 24–40.

^[2] E. Rosenberg, K. I. Hardcastle, *Comprehensive Organometallic Chemistry II*, Pergamon, **1995**, vol. 10, chapter 6, p. 323 and references therein.

^[3] V. G. Albano, D. Braga, S. Martinengo, *J. Chem. Soc., Dalton Trans.* **1986**, 981–984.

^[4] V. G. Albano, D. Braga, S. Martinengo, *J. Chem. Soc., Dalton Trans.* **1981**, 717–720.

^[5] B. T. Heaton, L. Strona, S. Martinengo, *J. Organomet. Chem.* **1981**, *215*, 415–422.

^[6] S. Martinengo, D. Strumolo, P. Chini, V. G. Albano, D. Braga, *J. Chem. Soc., Dalton Trans.* **1985**, 35–41.

^[7] A. Fumagalli, S. Martinengo, V. G. Albano, D. Braga, *J. Chem. Soc., Dalton Trans.* **1988**, 1237–1247.

^[8] B. T. Heaton, L. Strona, S. Martinengo, D. Strumolo, V. G. Albano, D. Braga, *J. Chem. Soc., Dalton Trans.* **1983**, 2175–2182.

^[9] See, for example: ^[9a] P. Braunstein, J. Rosé, A. M. Manotti-Lanfredi, A. Tiripicchio, *J. Chem. Soc., Dalton Trans.* **1984**, 1843–1848. – ^[9b] C. P. Horwitz, E. M. Holt, C. P. Brock, D. F. Shriver, *J. Am. Chem. Soc.* **1985**, *107*, 8136–8146. – ^[9c] O. Rossell, M. Seco, R. Reina, *Organometallics* **1994**, *13*, 2127–2130. – ^[9d] O. Rossell, M. Seco, G. Segalés, S. Alvarez, M. A. Pellinghelli, A. Tiripicchio, *Organometallics* **1994**, *13*, 2205–2212. – ^[9e] R. Reina, O. Rossell, M. Seco, D. de Montauzon, R. Zquiak, *Organometallics* **1994**, *13*, 4300–4305.

^[10] R. Reina, O. Riba, O. Rossell, M. Seco, P. Gómez-Sal, A. Martín, *Organometallics* **1997**, *16*, 5113–5115.

^[11] R. Reina, O. Rossell, M. Seco, *J. Organomet. Chem.* **1990**, *398*, 285–291.

^[12] P. Braunstein, J. Rosé, A. Tiripicchio, M. Tiripicchio-Camellini, *J. Chem. Soc., Dalton Trans.* **1992**, 911–920.

^[13] D. M. P. Mingos, D. J. Wales, *Introduction to Cluster Chemistry*, Prentice Hall International, London, **1990**.

^[14] See, for example: ^[14a] Y. Yamamoto, H. Yamazaki, T. Sakurai, *J. Am. Chem. Soc.* **1982**, *104*, 2329–2330. – ^[14b] P. Braunstein, J. Rosé, A. Tiripicchio, M. Tiripicchio-Camellini, *Angew. Chem. Int. Ed. Engl.* **1985**, *24*, 767–768. – ^[14c] Y. Yamamoto, H. Yamazaki, *Inorg. Chim. Acta* **1994**, *217*, 121–127. – ^[14d] L. H. Gade, B. F. G. Johnson, J. Lewis, M. McPartlin, I. J. Scowen, *J. Chem. Soc., Dalton Trans.* **1996**, 597–601.

^[15] O. Rossell, M. Seco, G. Segalés, M. A. Pellinghelli, A. Tiripicchio, D. de Montauzon, *Organometallics* **1997**, *16*, 236–245.

^[16] R. Reina, O. Riba, O. Rossell, M. Seco, P. Gómez-Sal, A. Martín, D. de Montauzon, A. Mari, *Organometallics* **1998**, *17*, 4127–4135.

^[17] R. Reina, O. Riba, O. Rossell, M. Seco, unpublished results.

^[18] P. Lemoine, A. Giraudeau, M. Gross, R. Bender, P. Braunstein, *J. Chem. Soc., Dalton Trans.* **1981**, 2059–2062.

^[19] J. Rimmelin, P. Lemoine, M. Gross, R. Mathieu, D. de Montauzon, *J. Organomet. Chem.* **1986**, *309*, 363–367.

^[20] M. J. Mays, J. D. Robb, *J. Chem. Soc., A* **1968**, 329–332.

^[21] P. Cassoux, R. Dartiguepeyron, D. de Montauzon, J. B. Tommasino, P. L. Fabre, *Actual Chim.* **1994**, *1*, 49–55.

^[22] G. M. Sheldrick, *SHELXL-97*, Universität Göttingen, **1997**.

^[23] *International Tables of X-ray Crystallography*, Kynoch Press, Birmingham, **1974**, Vol. IV, p. 99–100 and 149.

Received June 15, 2000
[I00243]